Turkish Journal of Electrical Engineering & Computer Sciences

http://journals.tubitak.gov.tr/elektrik/

Research Article

Turk J Elec Eng & Comp Sci
(2017) 25: 4445 – 4456

doi:10.3906/elk-1704-140

A novel microstrip diplexer design with tunable bandwidths and switchable channels for 4.5G applications

Ali Kürşad GÖRÜR[1,*], Pınar ÖZTÜRK ÖZDEMİR[2], Elif GÜNTÜRKÜN ŞAHİN[3], Ceyhun KARPUZ[2]

[1]Department of Electrical and Electronics Engineering, Faculty of Engineering and Architecture, Nevşehir Hacı Bektaş Veli University, Nevşehir, Turkey

[2]Department of Electrical and Electronics Engineering, Faculty of Engineering, Pamukkale University, Denizli, Turkey

[3]Department of Electrical & Electronics Engineering, Faculty of Engineering, Ömer Halisdemir University, Niğde, Turkey

Received: 12.04.2017 • **Accepted/Published Online:** 22.08.2017 • **Final Version:** 03.12.2017

Abstract: In this paper, a novel microstrip diplexer with tunable bandwidths and switchable channels is presented by using dual-mode square loop resonators (DMSLRs). Two resonators at different electrical lengths are coupled to input and output ports with lumped capacitors, and the isolation between the output ports is optimized by means of these capacitors. In order to obtain tunable bandwidth in each channel, varactor diodes are located at the orthogonal corners of the proposed resonators. In addition, the proposed resonators have reference patch elements at the lateral arms to provide convenience of varactor diode capacitances, such as perturbation elements. Depending on the capacitances of the varactor diodes, the bandwidths of each channel can be tuned. Furthermore, each channel can be switched off. The designed diplexer has two channels at the center frequencies of 1.8 and 2.6 GHz, which are allocated to 4.5G applications. Three-dB bandwidths can be tuned between 60 and 160 MHz for the first channel and between 150 and 350 MHz for the second channel. Isolation between the output ports is obtained as better than 18 dB in each channel. The designed diplexer was fabricated and measured, and the measured results were consistent with the predicted results.

Key words: Diplexer, microstrip, tunable, bandwidth, dual-mode resonator

1. Introduction

In recent years, owing to the rapid developments in space and satellite communication systems, microwave multiplexers have been acquiring a great significance, since they can provide multiple frequency bands at different outputs. Consequently, microwave multiplexers with suitable operating frequencies for Wi-Fi, WLAN, WiMAX, 3G, 4G, 4.5G, and 5G are widely used in wireless communication systems. Planar structures, such as microstrip, coplanar waveguides, and coplanar striplines are greatly preferred in microwave multiplexer design due to their low loss and cost, easy fabrication, compactness, etc. Among these, microstrip is the most preferred structure type, and is frequently used in multimode, multiband, and tunable filters [1–6]. To date, many microstrip diplexers or triplexers have been studied by various researchers [7–13]. These works have focused on obtaining multiple channels, low insertion losses at all channels, and high isolation between the output ports [8–13].

Although there are many studies on microstrip diplexers or triplexers, the number of tunable multiplexers

*Correspondence: kgorur@nevsehir.edu.tr

is quite low. In [14], an electronically tunable diplexer was designed for frequency agile transceiver front-end. A tunable passband can be obtained at the transmit and receive channels of the front-end. Another microstrip diplexer with tunable center frequency was designed in [15]. The designed filter has three poles at each channel and allows tuning each channel independently in terms of center frequency. Open loop ring resonators and dual-mode stub-loaded resonators have additionally been utilized in tunable microstrip design [16,17]. Furthermore, a switching technique for diplexers has been used to design a bandpass filter with a wide center frequency tuning range [18]. This study includes both a tunable diplexer and a bandpass filter with a wide tuning range. In another study, a reconfigurable matching network implementation was realized, and a tunable diplexer with tunable center frequency at two outputs was demonstrated [19]. A four-channel microstrip switchable diplexer, using joint T-shaped resonators, was introduced in [20].

Bandwidth tunability at each channel is an important issue for tunable microstrip diplexers. A dual-mode ring resonator topology is the most suitable way to design a microstrip diplexer with tunable bandwidth, since it can provide bandwidth enhancement due to the perturbation element, as described in [21,22].

This paper presents a novel microstrip diplexer design with tunable bandwidth and switchable channels for 4.5G applications. The proposed diplexer is constructed by using DMSLRs with varactor diodes, which serve as perturbation elements. Two DMSLRs with different electrical lengths are used to obtain two channels located at 1.8 GHz and 2.6 GHz. Both resonators are coupled to input and output ports by lumped capacitors. The lumped capacitors are effective in the isolation between the output ports. The bandwidth of both channels can be tuned according to the capacitances of the varactor diodes located. Both channels can be switched off independently by means of the varactor diodes. The designed tunable microstrip diplexer has been fabricated and measured for experimental verification. The measured results show a good agreement with the predicted results. Whereas the first channel at 1.8 GHz has a bandwidth tuning range between 60 and 160 MHz, the bandwidth of the second passband at 2.6 GHz can be tuned from 150 to 350 MHz.

2. Resonator analysis

The proposed resonator configuration is illustrated in Figure 1a. It is coupled to the input and output ports by coupling capacitors, C_g. As can be seen, a varactor diode as a tuning element and two reference patch elements are used. Equivalent circuit models under even and odd mode excitations of the proposed resonator are depicted in Figures 1b and 1c, respectively. It is obvious that input capacitor C_g is not taken into account in the equivalent circuit models, since the latter only describe the characteristics of the proposed resonator. In Figure 1b, both the reference elements and the varactor diodes are represented, since the symmetrical axis of the resonator is short-circuited under even mode excitation. Hence, even mode resonance condition has to include both capacitances of reference elements and varactor diodes. Based on Figure 1b, even mode input admittance can be expressed as follows:

$$Y_{even} = jY_0 \frac{(1-\tan(\theta)^2)(b_r + b_p + Y_0\tan(2\theta) - \frac{b_r b_p \tan(2\theta)}{Y_0}) + 2\tan(\theta)(Y_0 - b_p\tan(2\theta))}{Y_0 - b_p\tan(2\theta) - b_p\tan(\theta) - Y_0\tan(\theta)\tan(2\theta) - b_r\tan(\theta) + b_r b_p\tan(\theta)\tan(2\theta)}, \quad (1)$$

where Y_0 is the characteristic admittance of the transmission line in the resonator, and $b_p = wC_p$ and $b_r = wC_r$ represent the susceptances of perturbation and reference capacitances. In addition, θ is the electrical length of the related transmission line, which can be calculated with the multiplication of the propagation constant and physical length of the transmission line. Even mode resonance condition can be found by equating Y_{even} to 0,

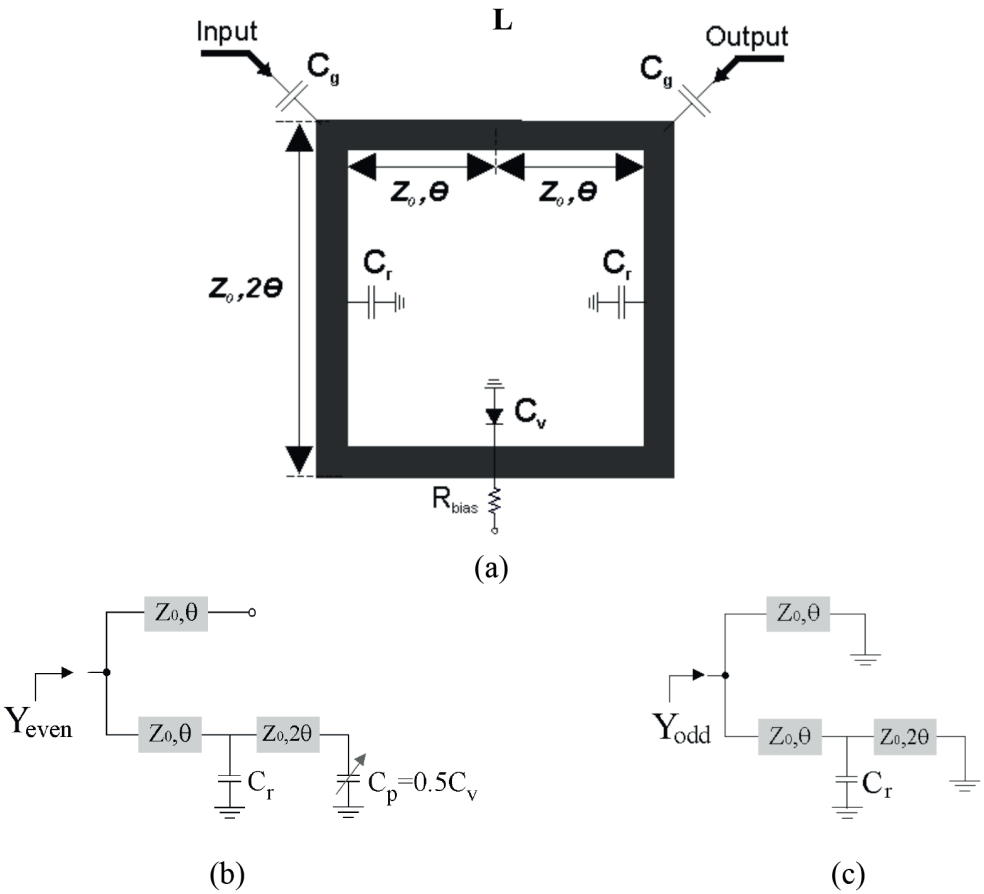

Figure 1. a) Proposed dual-mode resonator, b) even-mode equivalent circuit of the proposed resonator, c) odd-mode equivalent circuit of the proposed resonator.

as in [7]:

$$b_r \cot(2\theta) + 2b_p \cot(4\theta) + 2Y_0 - \frac{b_r b_p}{Y_0} = 0 \tag{2}$$

According to Figure 1c, since the varactor diode is short-circuited in the odd mode equivalent circuit model, the odd mode resonance condition does not need to include the capacitance of the varactor diode. Odd mode input admittance can be formulated as follows:

$$Y_{odd} = jY_0 \frac{2b_r - 2Y_0 \cot(2\theta) + Y_0 \tan(\theta) - Y_0 \cot(\theta)}{Y_0 - b_r \tan(\theta) + Y_0 \tan(\theta) \cot(2\theta)} \tag{3}$$

In a similar manner, with even mode excitation, the odd mode resonance condition can be expressed by equating Y_{odd} to 0, as follows:

$$Z_0 b_r = 2 \cot(2\theta) \tag{4}$$

From the numerical solutions of Eqs. (2) and (4), even and odd mode resonance frequencies can be derived, respectively. The center frequency of the passband can be calculated by meaning those values arithmetically as

$$f_c = \frac{f_{even} + f_{odd}}{2}, \tag{5}$$

where f_{even} and f_{odd} are even- and odd-mode resonance frequencies calculated from Eqs. (2) and (4). Thus, we can obtain the center frequency of a passband, constructed by the proposed resonator. This center frequency determination approach has been previously applied in the literature [23]. In addition, bandwidth of the passband can be tuned by changing f_{even} by means of a variable capacitor such as a varactor diode. In a dual-mode resonator, whereas even- and odd-mode resonance frequencies are almost equal, switching operation can be obtained as described in [21].

3. Microstrip diplexer design

By coupling the proposed resonator to input and output ports, a microstrip multiplexer can be designed. As shown in Figure 2, two resonators of different electrical lengths are coupled to input and output ports by means of lumped capacitors C_{g1} and C_{g2}, in order to obtain a microstrip diplexer structure. Perturbation capacitance, represented as C_p in the previous section, is renamed as C_v, since varactor diodes are used instead of perturbation elements. Therefore, C_{v1} and C_{v2} are the varactor diode capacitances for the first and second resonators, respectively.

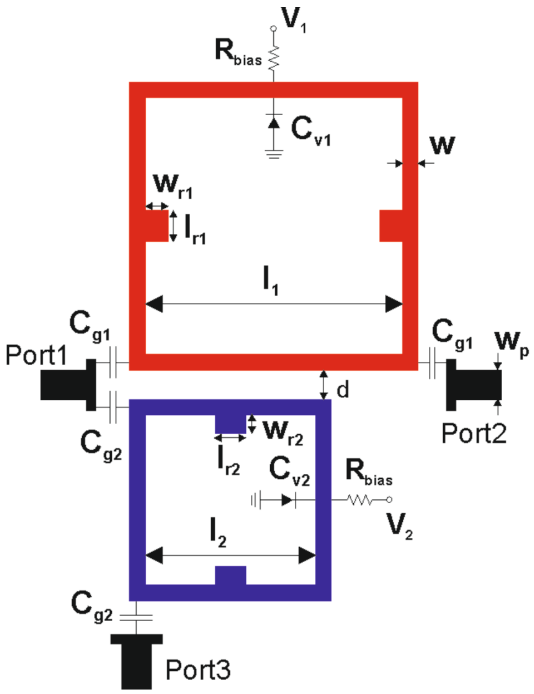

Figure 2. Designed tunable microstrip diplexer.

An RT/Duroid substrate (Rogers RT6006) with a thickness of 1.27 mm, a relative dielectric constant of 6.15, and a dielectric tangent loss of 0.0027 are used in all design processes. Reference capacitors are represented with patch elements having dimensions of l_r and w_r. Capacitances of lumped capacitors are assigned by optimizing the frequency response of the proposed diplexer in a full-wave electromagnetic simulator [24]. The main optimization goals can be ordered as follows:

1. Obtain the best isolation level between the output ports.
2. Obtain the best insertion loss levels at passbands.

3. Obtain the maximum bandwidth tuning range with the previous ones.

4. Adjust the center frequencies of the passbands to 1.8 and 2.6 GHz.

The dimensions of the designed diplexer are given in Table 1. These dimensions are selected to adjust the center frequencies of two channels to 1.8 and 2.6 GHz, which are applicable to 4.5G systems. Center frequencies can be calculated according to the method described in the previous section. In other words, all dimensions can be approximately found from the numerical solutions of Eqs. (2) and (4). Furthermore, it should be noted that the electrical length θ approximately corresponds to $l_1/2$ or $l_2/2$ for the first and second channels, respectively. The lengths of patch reference elements, l_{r1} and l_{r2}, are chosen as equal in order to adjust the capacitances of those elements by only changing the widths w_{r1} and w_{r2}. Input and output ports are adjusted to 50 ohms, which requires a line width of 1.9 mm for the substrate utilized in design. Mutual coupling between the two resonators is negligible, since there is enough space between the neighbor transmission lines of the resonators (d = 1.9 mm).

Table 1. Dimensions of the designed diplexer (units: mm).

w_p	w	l_1	l_2	w_{r1}	l_{r1}	w_{r2}	l_{r2}	d
1.9	1.0	16.6	11.0	1.8	2.2	1.4	2.2	1.9

Bandwidth tuning operations and switching operations for both channels are represented in Figures 3a–3c. As shown in Figure 3a, the bandwidth of the first channel can be tuned due to the change in C_{v1}. A tuning range between 60 and 120 MHz can be achieved. The mentioned bandwidth belongs to 3-dB bandwidth. In this paper, bandwidth calculations are achieved due to the difference between the 3-dB intersection points S_{11} and S_{21} (or S_{31}). In Table 2, approximate numerical data (read from simulations) are shown at the significant capacitance values.

Table 2. Numerical values for the first channel tuning operation (simulations).

C_{v1} (pF)	f_{3dB1} (GHz)	f_{3dB2} (GHz)	IL (@ f_{3dB1}) (dB)	IL (@ f_{3dB2}) (dB)	BW (MHz) ($f_{3dB2} - f_{3dB1}$)	Min. IL (dB)
0.70	1.86	1.92	4.38	4.01	60	1.78
0.75	1.84	1.92	3.97	3.95	80	1.19
0.80	1.83	1.93	3.93	3.75	100	0.93
0.85	1.81	1.93	3.85	3.70	120	0.95

Insertion loss can be obtained as better than 2 dB, whereas in-band return loss varies between 10 and 20 dB. During the tuning operation, center frequency ranges from 1.84 to 1.88 GHz. This change results from the tuning mechanism, since it can only allow tuning in the even mode resonance frequency. Thus, odd mode is fixed at a frequency, and the center frequency of the passband is tuned according to Eq. (3). Figure 3b illustrates the tuning operation for the second channel due to the change in C_{v2}. The bandwidth of this channel can be tuned between 150 and 330 MHz with an insertion loss higher than 1.5 dB. In-band return loss varies between 10 and 20 dB. Similarly, center frequency fluctuates between 2.61 and 2.66 GHz during the tuning operation. Figure 3c illustrates the switching operation for both channels. As mentioned in the previous section, according to the capacitance of the varactor diode, both channels can be turned off. The first channel can be switched off while C_{v1} is 0.55 pF, and the second channel can be switched off while C_{v2} is 0.5 pF. Detailed numerical values

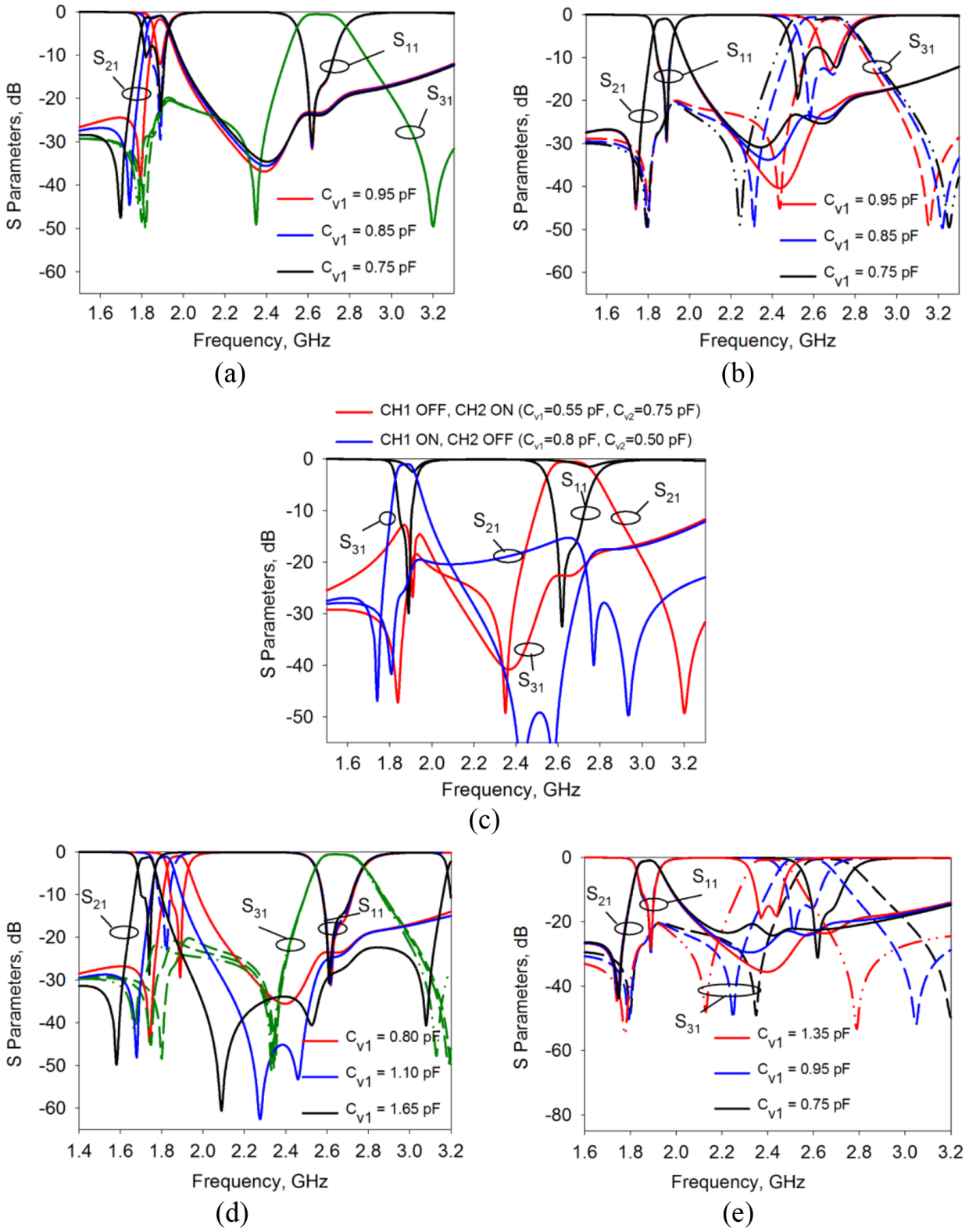

Figure 3. a) Tuning operations for the first channel (simulated), b) tuning operations for the second channel (simulated), c) switching operations of both channels (simulated), d) center frequency control for the first channel (simulated), e) center frequency control for the second channel (simulated).

for the second channel bandwidth tuning operation can be seen in Table 3. Center frequencies of the channels can be controlled by changing the dimensions of the reference patch elements and capacitances of the varactor diodes without changing the resonator dimensions. Figures 3d and 3e show the center frequency control against varactor diode capacitances as well as reference patch elements dimensions. For the first channel control, the total area of the reference patch element is varied as 24 × 48 mm^2, 22 × 28 mm^2, and 16 × 20 mm^2, whereas the capacitance of the varactor diode, C_{v1}, is varied as 1.65, 1.10, and 0.8 pF, respectively. For the second channel control, the dimensions of reference patch elements are varied as 30 × 30 mm^2, 22 × 20 mm^2, and 13 × 20 mm^2, whereas C_{v2} is varied as 1.35, 0.95, and 0.75 pF, respectively.

Table 3. Numerical values for the second-channel tuning operation (simulations).

C_{v1} (pF)	f_{3dB1} (GHz)	f_{3dB2} (GHz)	IL (@ f_{3dB1}) (dB)	IL (@ f_{3dB2}) (dB)	BW (MHz) ($f_{3dB2} - f_{3dB1}$)	Min. IL (dB)
0.65	2.60	2.75	3.84	3.59	150	1.01
0.70	2.57	2.77	3.80	3.50	200	0.64
0.80	2.52	2.78	3.66	3.45	260	0.60
0.90	2.46	2.79	3.65	3.44	330	0.60

In a microstrip diplexer design, isolation between the output ports must be maximized, since transmission between output ports is needed to be disallowed. The isolation of the designed diplexer is shown in Figure 4 against different coupling capacitances. Accordingly, isolation can be increased by decreasing the coupling capacitances. However, bandwidth tuning range decreases at the same time. In the frequency responses with narrower bandwidth, bandwidth tuning range is limited with the return loss levels and cannot be tuned in a wide range. Therefore, the balance between the isolation level and bandwidth tuning range should be maintained based on this trade-off. The best trade-off can be obtained while C_{g1} and C_{g2} are 0.5 pF.

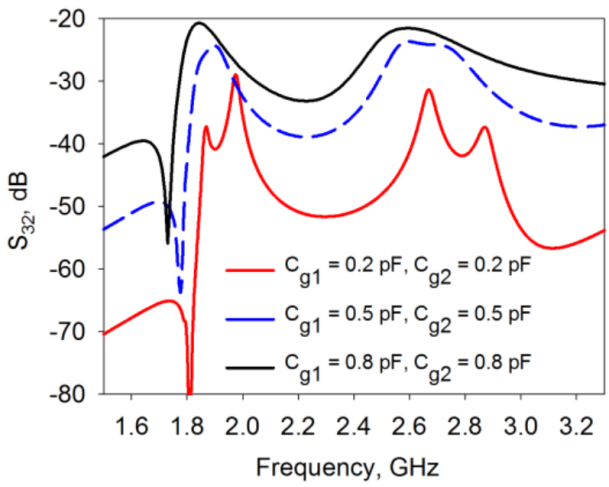

Figure 4. Isolation level adjustment due to the changes in coupling capacitances (simulated).

4. Experimental studies

In this section, the designed microstrip diplexer is fabricated and measured. A photograph of the fabricated diplexer is shown in Figure 5. Measurements were taken by using Agilent E5071C network analyzer. Infineon

BB857 varactor diodes were used to tune the diplexer. Additionally, AVX thin film capacitors were used to implement the lumped coupling capacitors utilized in the experiments. Varactor diodes are driven by bias resistors of 10 kΩ at both resonators. The total circuit size is 27.8 $\times$ 38.3 mm^2. This corresponds to 0.23 $\times$ 0.167 λ_g (0.038 λ_g^2), where λ_g is the guided wavelength at the lowest channel frequency of 1.8 GHz for the used substrate. The dimensions of the fabricated filter are the same as the simulated ones given in Table 1.

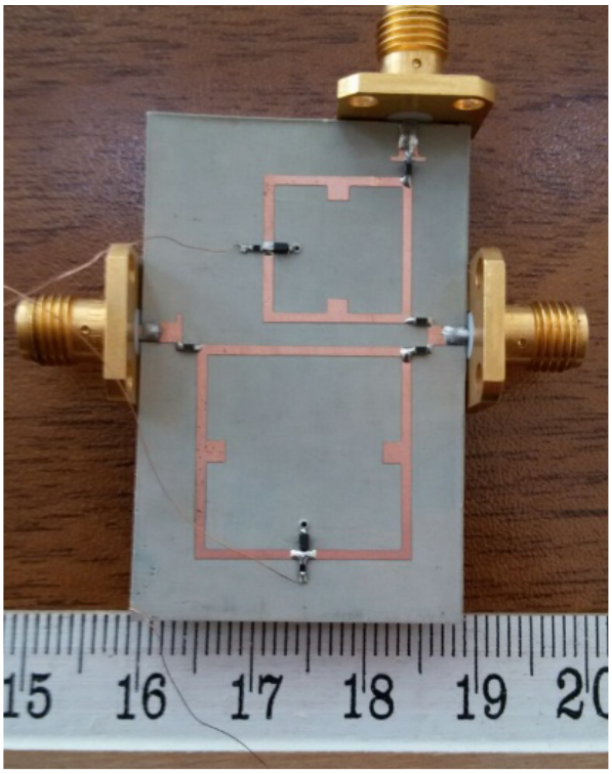

Figure 5. Photograph of the fabricated filter.

The measured results are demonstrated in Figures 6a and 6b. Figure 6a shows the bandwidth tuning operation for the first channel. As can be seen, bandwidth can be tuned towards low frequencies. Three-dB bandwidth can be tuned from 60 MHz to approximately 160 MHz. Bias voltages were applied between 13 and 20.8 V. During this operation, center frequency varies between 1.80 and 1.85 GHz. Insertion losses were observed as better than 3.5 dB in all tuning steps. When the bias voltage is 20.8 V, the highest insertion loss is measured as 3.47 dB. When it is 13 V, the highest insertion loss in the passband is observed as 2.75 dB. For the other tuning steps, insertion loss is consistently better than those values. Minimum insertion loss level is approximately 1.4 dB when the bias voltage is between 13 and 16 V. Return loss varies between 10 and 20 dB. The numerical results of the measurements according to the significant bias voltages for the first channel are given in Table 4. Figure 6b illustrates bandwidth tuning operation for the second channel. Similarly, 3-dB bandwidth can be tuned towards low frequencies with a tuning range of approximately 150–350 MHz. Applied bias voltages for this operation are between 14 and 22.8 V. Accordingly, center frequency varies between 2.52 and 2.63 GHz. Insertion losses are observed as better than 2.3 dB and return losses are obtained as better than 10 dB. The worst insertion loss is measured as 2.28 dB, whereas the bias voltage is 22.8 V. For other tuning steps, insertion loss level is always better than 1.8 dB. Each channel can be turned off according to the bias voltages of the varactor diodes. Turn-off operations for both channels are shown in Figure 6c. Turn-off ratios

are measured as better than 10 dB when the bias voltages for the first and second varactors are 27.8 and 28.2 V, respectively. Additionally, isolation between the output ports is measured as depicted in Figure 7, and is obtained as better than 18 dB at each channel frequency. The numerical results of the measurements according to the significant bias voltages for the second channel are given in Table 5.

Table 4. Numerical values for the first-channel tuning operation (measurements).

Bias Voltage (V)	f_{3dB1} (GHz)	f_{3dB2} (GHz)	IL (@ f_{3dB1}) (dB)	IL (@ f_{3dB2}) (dB)	BW (MHz) ($f_{3dB2} - f_{3dB1}$)	Min. IL (dB)
13.0	1.75	1.91	4.05	4.11	160	1.09
14.3	1.77	1.91	4.0	4.24	140	1.19
15.5	1.785	1.91	4.36	4.36	125	1.32
17.3	1.80	1.90	4.18	4.13	100	1.73
19.0	1.82	1.90	4.22	4.49	80	2.31
20.8	1.84	1.90	4.18	4.35	60	3.13

Table 5. Numerical values for the second channel tuning operation (measurements).

Bias Voltage (V)	f_{3dB1} (GHz)	f_{3dB2} (GHz)	IL (@ f_{3dB1}) (dB)	IL (@ f_{3dB2}) (dB)	BW (MHz) ($f_{3dB2} - f_{3dB1}$)	Min. IL (dB)
14.0	2.41	2.76	3.96	3.89	360	1.23
15.5	2.42	2.71	3.96	3.98	290	1.25
17.5	2.46	2.71	3.95	3.86	250	1.25
20.0	2.51	2.71	3.86	3.75	200	1.40
22.8	2.55	2.70	3.96	3.97	150	2.22

The designed structure has important novelties as compared to the electronically tunable diplexers in the literature in terms of tunable bandwidth and switchable characteristics at both channels. A comparison with similar works is given in Table 6. The designed diplexer allows us to both switch and tune each channel independently in terms of bandwidth. Therefore, this study proposes a novel approach for electronically tunable microstrip diplexer design methodologies with acceptable performances.

5. Conclusion

In this study, a novel microstrip diplexer with tunable bandwidth was designed, fabricated, and measured. The designed structure has two dual-mode resonators of different electrical lengths with reference patch elements located at the lateral arms, and a varactor diode instead of a perturbation element. Assignment of resonance frequencies for each channel was investigated by introducing even- and odd-mode resonance conditions. Both channels can be switched off by means of the proposed structure. The designed filter was fabricated and measured for the experimental verification of the simulated results in an acceptable agreement. Bandwidth tunability and switching operations were demonstrated in measurements. The designed microstrip diplexer is applicable for 4.5G systems, since it has two channels operating at 1.8–1.9 GHz and 2.6–2.7 GHz with tunable and switchable characteristics.

In future research, we will incorporate a center frequency tuning mechanism for both channels. For this purpose, two more varactor diodes are considered to be used instead of reference patch elements. Thus, we expect to obtain an electronic tuning mechanism for center frequency instead of dimension-based control, as

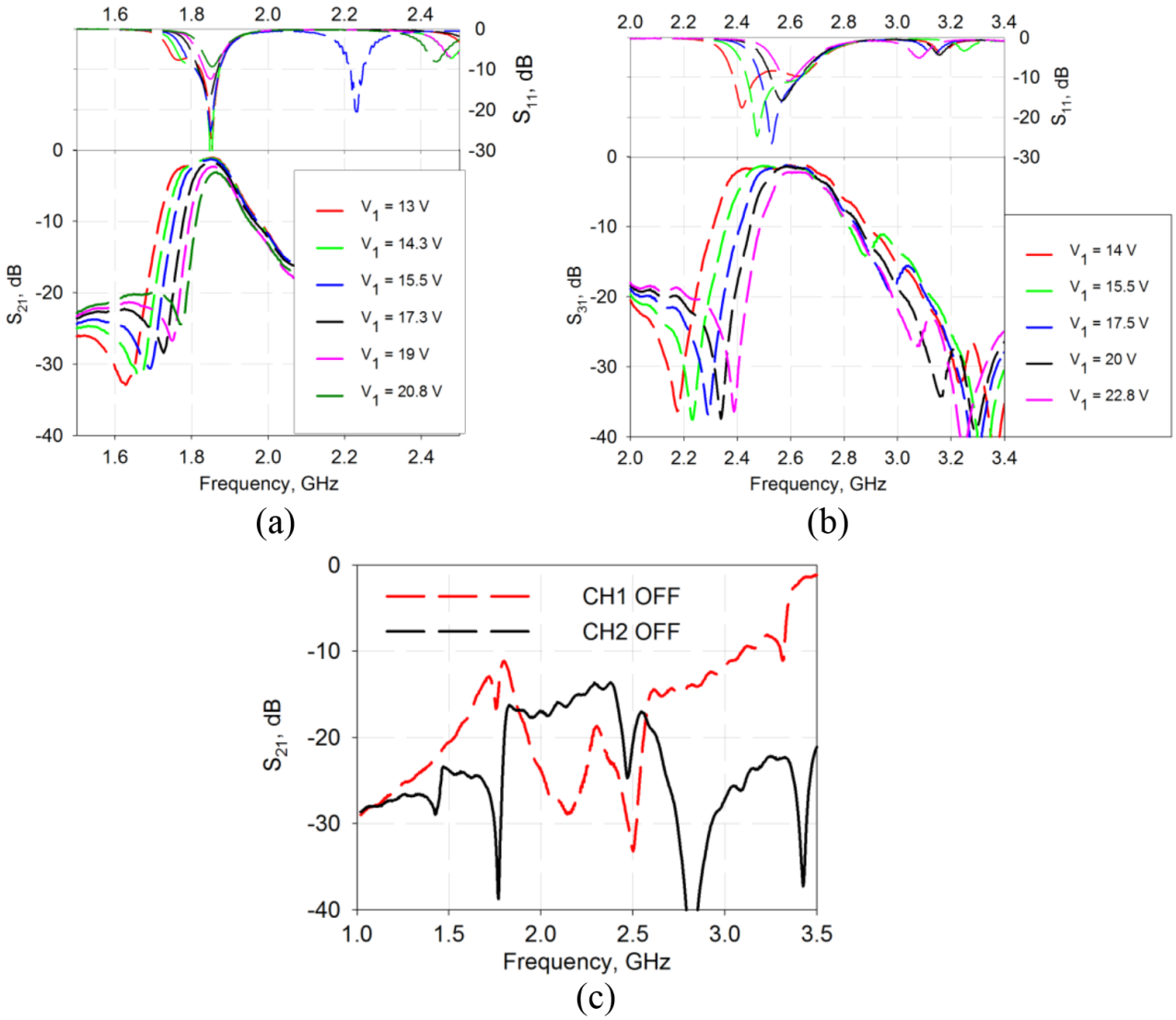

Figure 6. a) Tuning operations for the first channel (measured), b) tuning operations for the second channel (measured), c) switching operations of both channels (measured).

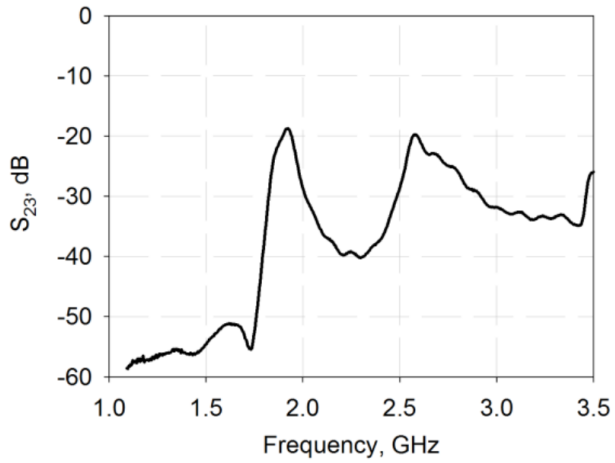

Figure 7. Measured isolation level between the output ports.

Table 6. Comparison with similar works (*CF: center frequencies).

References	IL variation (dB)	Size ($\lambda_g \times \lambda_g$)	Isolation (dB)	Tunable CF*	Switchable channels	Tunable bandwidth
[8]	1.46, 1.44	0.228	> 36	×	×	×
[9] (8 channel diplexer)	2.1 < ILv < 2.8 @ channels	0.1	> 29	×	×	×
[12]	3, 2.4	NA	> 33	×	×	×
[13]	< 3	0.017	> 32	×	×	×
[14]	2.89–5.3 3.7–5.3	NA	> 40	✓	×	×
[16]	1.5–3.2 1.6–3.5	0.027	> 22	✓	×	×
[17]	1.4–7.2	0.154	> 45	✓	×	×
[18]	2.5–4.35 3.6–7.72	0.00551	> 20	✓	✓	×
[19]	5–7.7	NA	> 13	✓	×	×
[20] (4 channel multiplexer)	1.1, 1.4, 1.3, 1.5 (fixed)	0.25	> 18	×	✓	×
This work	1.09–4.49 1.23–3.98	0.1683	> 18	×	✓	✓

given in Figures 3d and 3e. On the other hand, in order to improve the performance of the proposed diplexer, an additional dual-mode resonator stage should be located to increase the degree of the channels. Thus, higher selectivity can be obtained at both channels, and isolation levels can be improved. Moreover, size reduction of the proposed topology can be achieved by using a meandered dual-mode loop resonator instead of square loop resonators.

Acknowledgement

This work was supported by the Scientific and Technological Research Council of Turkey (TÜBİTAK) (Grant No. 215E099).

References

[1] Rezaei A, Noori L. Tunable microstrip dual-band bandpass filter for WLAN applications. Turk J Elec Eng & Comp Sci, 2017; 25: 1388-1393.

[2] Xu J. Compact second-order dual- and quad-band bandpass filters using asymmetrical stub-loaded resonator and uniform-impedance resonator. Microw Opt Technol Lett 2015; 57: 997-1003.

[3] Murmu L, Das S, Bage A. A compact tri-band bandpass filter using multi-mode stub-loaded resonator. In: IEEE 2016 Asia–Pacific Microwave Conference; 5–9 December 2016; New Delhi, India. New York, NY, USA: IEEE. pp. 1-4.

[4] Wei F, Huang QL, Li WT, Shi XW. A compact quad-band band-pass filter using novel stub-loaded SIR structure. Microw Opt Technol Lett 2014; 56: 538-542.

[5] Weng MH, Ye CS, Su YK, Lan SW. A new compact quad-band bandpass filter using quad-mode stub loaded resonator. Microw Opt Technol Lett 2014; 56: 1630-1632.

[6] Bage A, Das S. A frequency reconfigurable dual pole dual band bandpass filter for X-band applications. Prog Electromagn Res Lett 2017; 66: 53-58.

[7] Hong JS, Lancaster MJ. Microstrip Filters for RF/Microwave Applications. New York, NY, USA: Wiley, 2001.

[8] Chen CF, Lin CY, Tseng BH, Chang SF. High-isolation and high-rejection microstrip diplexer with independently controllable transmission zeros. IEEE Microw Compon Lett 2014; 12: 851-853.

[9] Tu WH, Hung WC. Microstrip eight-channel diplexer with wide stopband. IEEE Microw Compon Lett 2014; 11: 742-744.

[10] Peng HS, Chiang YC. Microstrip diplexer constructed with new types of dual-mode ring filters. IEEE Microw Compon Lett 2015; 1: 7-9.

[11] Deng HW, Zhao YJ, Fu Y, Ding J, Zhou XJ. Compact and high isolation microstrip diplexer for broadband and WLAN application. Prog Electromagn Res 2013; 133: 555-570.

[12] Shi J, Chen JX, Bao ZH. Diplexers based on microstrip line resonators with loaded elements. Prog Electromagn Res 2011; 115: 423-439.

[13] Chen CF. Miniaturized and high isolation microstrip diplexers based on the tri-mode stub-loaded stepped-impedance resonators. J Electromagnet Wave 2012; 26: 14-15.

[14] Djoumessi EE, Wu K. Electronically tunable diplexer for frequency-agile transceiver front-end. In: IEEE 2010 MTT-S International Microwave Symposium; 20–28 May 2010; Anaheim, CA, USA. New York, NY, USA: IEEE. pp. 1.

[15] Yang T, Rebeiz GM. Three-pole 1.3–2.4-GHz diplexer and 1.1–2.45-GHz dual-band filter with common resonator topology and flexible tuning capabilities. IEEE T Microw Theory 2013; 10: 3613-3624.

[16] Chen CF, Lin CY, Tseng BH, Chang SF. A compact tunable microstrip diplexer using varactor-tuned dual-mode stub-loaded resonators. In: IEEE 2014 MTT-S International Microwave Symposium; 1–6 June 2014; Tampa, FL, USA. New York, NY, USA: IEEE. pp. 1-3.

[17] Feng W, Zhang Y, Che W. Tunable dual-band filter and diplexer based on folded open loop ring resonators. IEEE T Circuits-II 2016; 99: 1.

[18] Xu J, Zhu Y. Tunable bandpass filter using a switched tunable diplexer technique. IEEE T Ind Electron 2017; 4: 3118-3126.

[19] Ko CH, Rebeiz GM. A 1.4–2.3-GHz tunable diplexer based on reconfigurable matching networks. IEEE T Microw Theory 2015; 5: 1595-1602.

[20] Chuang ML, Wu MT. Microstrip multiplexer and switchable diplexer with joint T-shaped resonators. IEEE Microw Compon Lett 2014; 5: 309-311.

[21] Gorur A. Description of coupling between degenerate modes of a dual-mode microstrip loop resonator using a novel perturbation arrangement and its dual-mode bandpass filter applications. IEEE T Microw Theory 2004; 2: 671-677.

[22] Karpuz C, Gorur AK, Basmaci AN. Design of tunable microstrip dual-mode bandpass filter having reconfigurable filtering characteristics for mobile applications. In: IEEE 2016 European Microwave Conference; 4–6 October 2016; London, UK. New York, NY, USA: IEEE. pp. 647-650.

[23] Lei MF, Wang H. An analysis of miniaturized dual-mode bandpass filter structure using shunt-capacitance perturbation. IEEE T Microw Theory 2005; 53: 861-867.

[24] Sonnet Software. Sonnet User's Manual v. 14. North Syracuse, NY, USA: Sonnet Software, 2011.